Adsorption (2024) 30:1205–1212
https://doi.org/10.1007/s10450-024-00500-8

Water adsorption on amorphous carbon nitride thin films synthesized by pulsed laser deposition

Kamal Kayed[1]

Received: 24 April 2024 / Revised: 15 May 2024 / Accepted: 22 May 2024 / Published online: 1 June 2024

Abstract
In this work, we investigate the structural parameters that affect water adsorption on amorphous carbon nitride thin films synthesized by pulsed laser deposition. The study includes the case of ablation of graphite targets within molecular nitrogen and within a stream of nitrogen plasma afterglow. The results obtained showed that, the effect of Csp^2-Csp^2 bonds concentration on the adsorption of water molecules depends strongly on the ratio and distortion of the hexagonal rings. Furthermore, analysis of the spectral data showed that, the relationship between the hydrogen bonding strength of water molecules with the film surface and the concentration of Csp^2-Csp^2 bonds takes a specific mathematical formula in the case of structures composed mainly of hexagonal rings.

Keywords Laser deposition · Amorphous carbon nitride · Thin films · Adsorption · Hexagonal rings · FT-IR spectroscopy

1 Introduction

The phenomenon of water adsorption on carbon materials has received increasing attention from research groups around the world due to the effect of humidity on the properties of these materials. Humidity negatively affects their industrial applications [1–7]. Most studies dealing with this topic have been concerned with the distinct nature of directional interactions between water molecules as well as between water molecules and different polar groups present on the surface of the material [2].

Amorphous carbon nitride films have many important industrial applications in the fields of optoelectronics, photocatalysis, gas sensors, magnetic storage devices, computer drive systems, etc [8–12]. . . The performance of devices whose working mechanism involves the use of carbon nitride is highly affected by humidity. For example, humidity affects the tribological performance of the head disk interface in magnetic data storage devices [1].

Humidity causes the adsorption of water on the surface of the solid material, causing water molecules and water vapor to stick to the surface of the material, through either weak physical forces or stronger chemical forces [2, 13, 14]. Many studies [1, 2, 15–18] have proven that water adsorption on the surfaces of carbon nitride films is greatly affected by the chemical composition of these films. On the other hand, it was found that the microstructure affects the adsorption level. For example, based on electron paramagnetic resonance measurements, E. Broitman et al. [1] found that, amorphous carbon nitride films absorb significantly more water than booth fullerene-like carbon nitride films and a-C(sp^2). The same study showed that a-C(sp^2) adsorbs more than 14 times the amount adsorbed by FL-CNx. The lower water adsorption in FLCNx films was mainly explained by the lower probability of dangling bonds on the film surface [1].

The mechanism of water absorption in carbon materials involves the adsorption of water molecules on functional groups located at the junctions between the basal planes adjacent to the graphene layers. This results in the growth of water aggregates around the functional groups and then the adjacent aggregates bridge to form condensates, which eventually fill the confined space, and the extent of this pores filling depends on the size of the confined space [18, 19]. In this work, we explore in depth the factors that affect

✉ Kamal Kayed
khmk2000@gmail.com;
kamal.kayed2@damascusuniversity.edu.sy

[1] Department of physics, Faculty of Science, Damascus University, Damascus, Syria

Table 1 The parameters of the laser beam that was used to ablate graphite targets

Laser wavelength	Pulse duration	Laser fluence	Incidence angle	Deposition time
1064 nm	20 ns	12.8 J cm^{-2}	45°	30 min

Table 2 The deposition pressure for each prepared sample

	Sample code	Pressure [Pa]
Series A	a	10
	b	100
	c	300
	d	500
	e	1000
Series B	f	10
	g	100
	h	300
	i	500
	j	1000

water adsorption on amorphous carbon nitride films in order to determine the role of carbon microstructures, the ratio of hexagonal rings in the film, the degree of distortion of these rings, and the energy band gap in the overall mechanism of water adsorption.

2 Experimental

2.1 Sample preparation

Carbon nitride thin films (a-CN_x) were deposited on n-type Si (100) substrates in a Pyrex chamber by ablation of high-purity graphite targets using a pulsed laser beam generated by RD-YG-300 system. Deposition processes were carried out at various pressures of molecular nitrogen (series A) and nitrogen plasma afterglow (series B). Nitrogen plasma afterglow (NPA) generated by Microwave SAIREM GMP 20 KEDS at fixed transmitted power of 1000 W. Table 1 contains the parameters of the laser beam that was used to ablate graphite targets.

More important details about the technique and deposition procedures (especially the nitrogen plasma generation method) have been explained in previous works [10–12].

Table 2 contains the deposition pressure for each prepared sample.

2.2 Sample characterization

Infrared absorption spectra (FTIR) of a- CN_x films were achieved using a Bruker Vertex 7 Fourier transform infrared spectrophotometer with resolutions equal to 4 cm^{-1}.

Micro-Raman backscattering spectra of the films were recorded on a Jobin-Yvon T64000 operating with a 514.5 nm line of argon laser as the excitation source and a resolution of 2 cm^{-1}.

The optical band gap of the prepared films was calculated for all films (deposited on glass substrates) using the transmission spectra in the region 350 nm to 1000 nm obtained, using a Specords 100 Analytikjena AG UV-VIS-NIR spectrophotometer.

3 Results and discussion

Figure 1 shows the FTIR spectra of the prepared carbon nitride thin films (series A and B). It can be seen that the effect of pressure in the case of A series is limited to the intensity changes of the features. In the case of the B series, the intensity change is accompanied by the appearance of new features in the region of high wavenumbers. On the other hand, it appears that using nitrogen plasma leads to

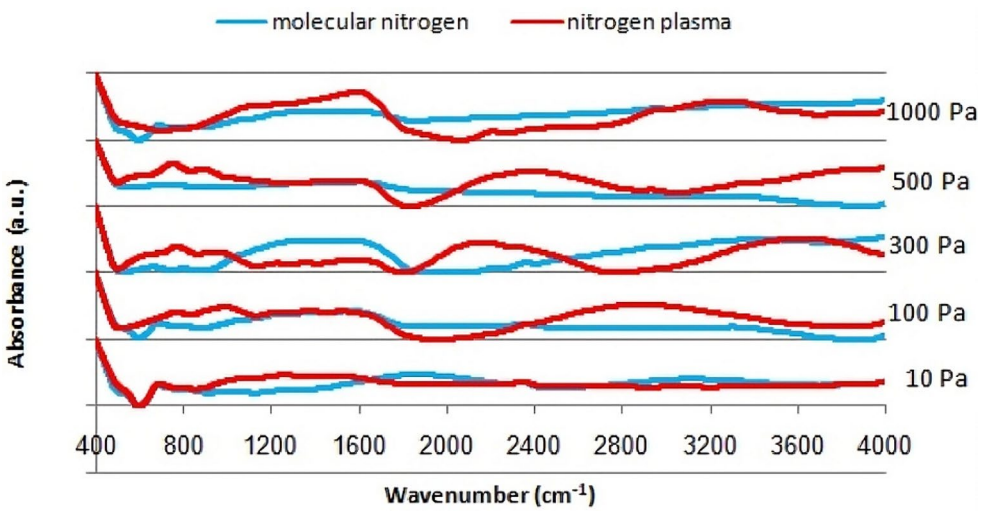

Fig. 1 The deconvoluted OH-group absorption peak for the sample **h** (300 Pa/series B)

Table 3 The chemical bonds and the vibrational patterns observed in the prepared thin films using FTIR spectroscopy

Number	Wavenumber (cm^{-1})	Chemical bond	References
1	2190	N = C = N	[10]
2	702	C-C-C deformations vibrations	[10]
3	843	C–C–N symmetric stretching vibrations	[10]
4	1000–1800	Appear as a result of the breaking of symmetry in carbon network	[10]
5	1600	C = N	[10]
6	1440 and 2900	CH_3.	[10]
7	2360	Atmospheric CO_2	[10]
10	2960	C-H stretching vibrations	[10]
11	3320	OH-group stretching vibrations in adsorbed water molecules	[10]

significant structural changes compared to the case of using molecular nitrogen.

Table 3 includes the wavenumbers and the chemical bonds (vibrational patterns) of the features appearing in the FTIR spectra of all samples (Fig. 2).

The effect of both nitrogen gas pressure and nitrogen plasma on the H-bonded H_2O in a-CN thin films can be investigated by analyzing the OH-group stretching vibrations peak that appear in the range 3000–4000 cm^{-1} in FTIR spectra of our samples. To achieve this, each OH-group peak was deconvoluted into two Gaussian-Lorentzian line shapes using Peak fit-4 software. As an example, the output of the deconvolution process for the sample **h** (300 Pa/series B) is illustrated in Fig. 1. We notice that the deconvolution results in two peaks S and W. The S peak belongs to the stronger bonded adsorbed water molecules, while the W peak belongs to the weaker bonded adsorbed water molecules. The reason for the decomposition of the original peak into two peaks (S and W) is the presence of two groups of water molecules. The first is responsible for the formation of the W peak and consists of free water vapor molecules ($(H_2O)_n$) adsorbed from the surrounding atmosphere. The second group is responsible for the formation of the S peak and consists of water molecules bond to the surface of the film by hydrogen bonds of the form $HOH.CN_x$.

Figure 3 illustrates the OH-group absorption peak area (S + W) as a function of deposition pressure. It can be seen that, in the case of molecular nitrogen (series A), the total area decreases with increasing deposition pressure. This means that, increasing deposition pressure leads to a decrease in the humidity of the sample. In the case of nitrogen plasma (series B), there is no specific behavior for the total area, and its maximum value reaches at 300 Pa (sample **h**). This sample is the most water adsorbent compared to the rest of the samples. The reason for this is that this sample has a high degree of deformation of the hexagonal rings [20], which provides interstitial spaces (pores) that help to absorb larger amounts of water compared to the rest of the samples. This is confirmed by the high FWHM value of the D band in the Raman spectrum of this sample (Fig. 4).

The S peak position (which belongs to water molecules bound to the film surface by hydrogen forces) depends on the strength of these bonds. Figure 5 shows the S peak position as a function of the deposition pressure. We notice that, the peak position for both types of samples reaches a maximum at a pressure of 100 Pa. Above this pressure, the position becomes oscillatory in the case of series A samples and decreases with increasing pressure in the case of series B samples. Based on the careful investigation of the structure

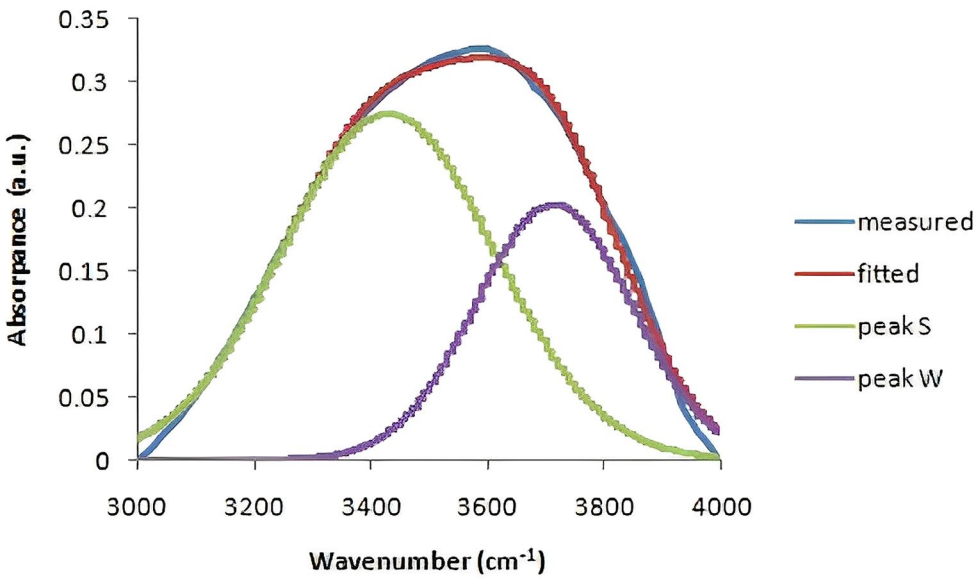

Fig. 2 The FTIR spectra of the prepared carbon nitride thin films (series **A** and **B**)

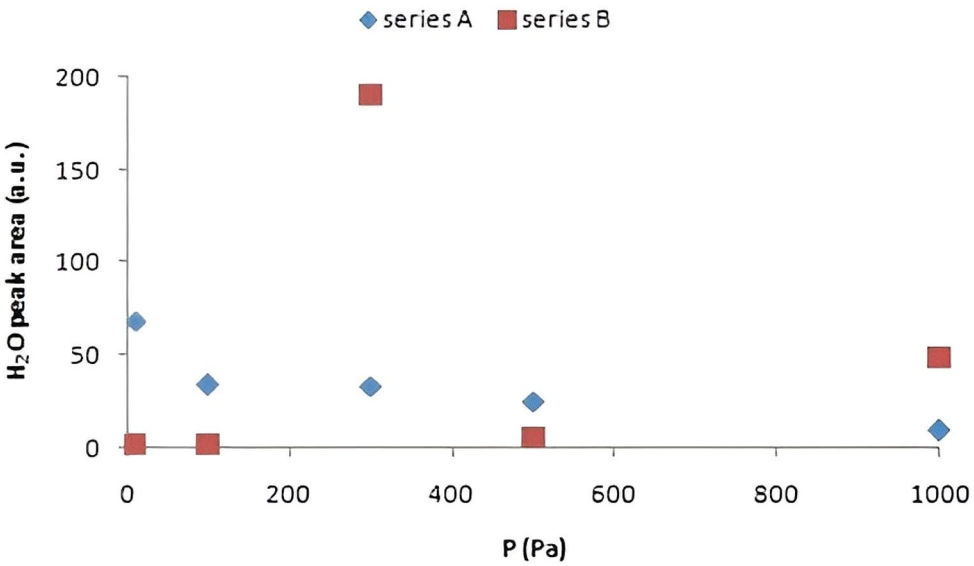

Fig. 3 The total area of the peaks S and W as a function of deposition pressure

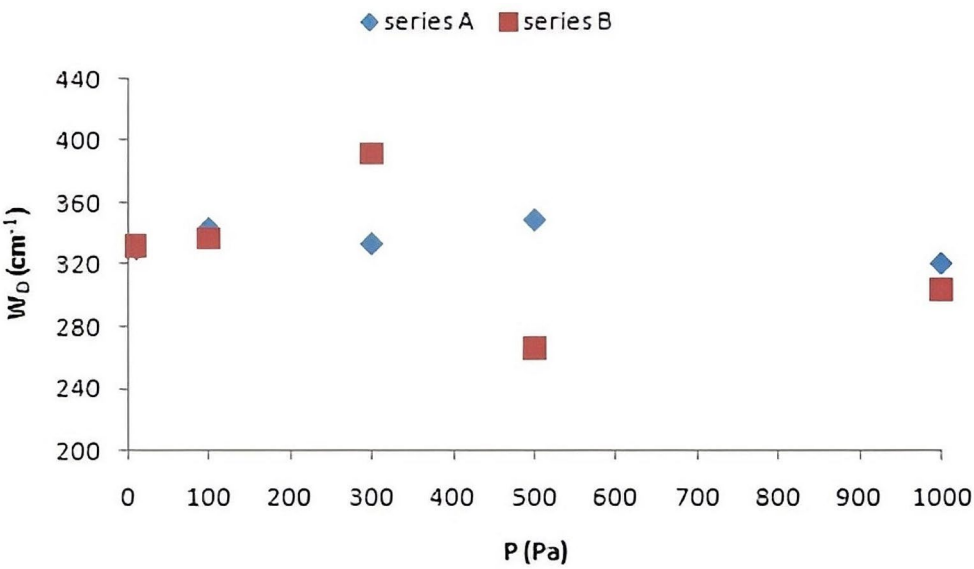

Fig. 4 The D band spectral width as a function of deposition pressure

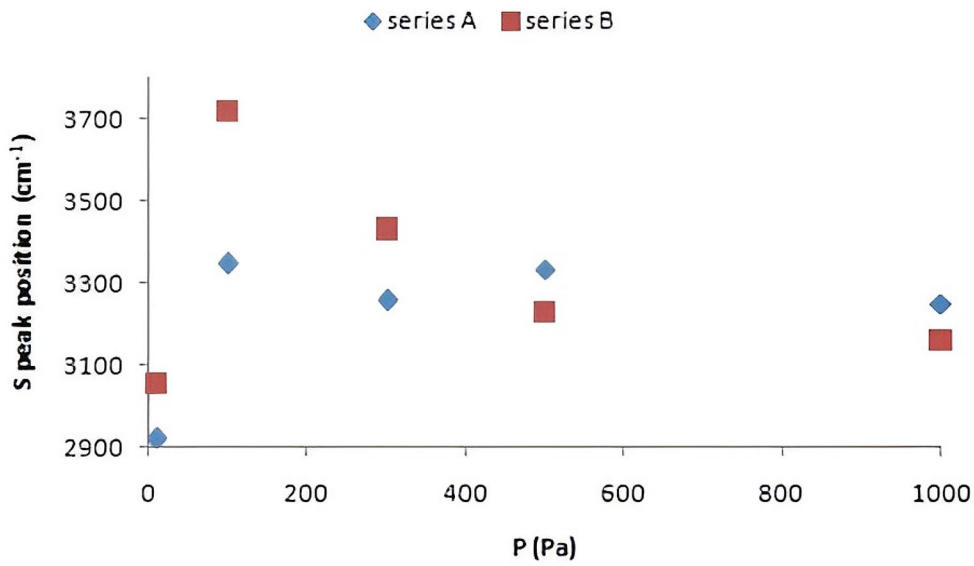

Fig. 5 The S peak position as a function of the deposition pressure

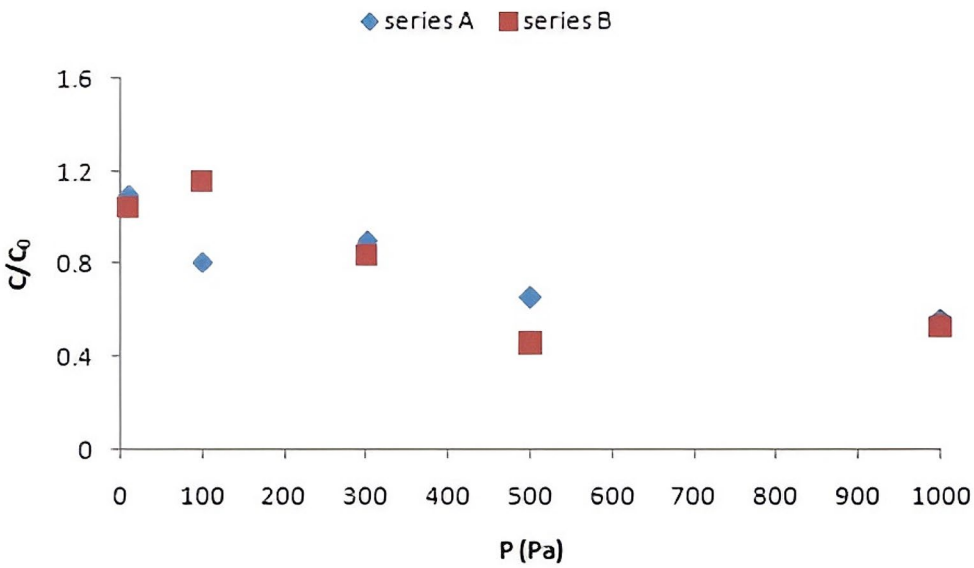

Fig. 6 The ratio C/C_0 as a function of the deposition pressure

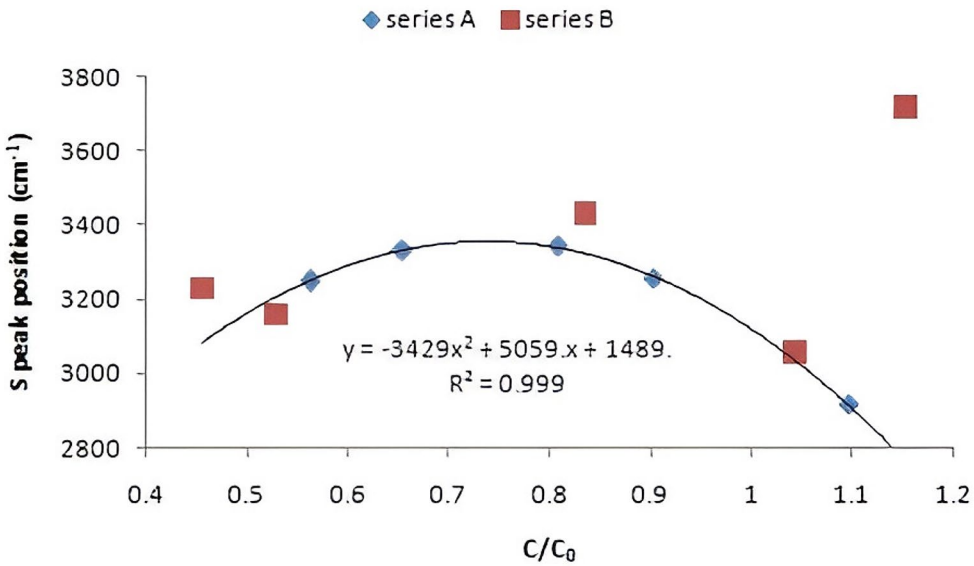

Fig. 7 The S peak position as a function of the ratio C/C_0

of our samples performed in previous works [10, 11], we can assume that the behavior of the two curves in Fig. 5 is controlled by two factors:

- The hexagonal rings distortion degree. This factor is related to the spectral width of the D peak in Raman spectra.
- The percentage of Csp^2-Csp^2 bonds in the film. We will symbolize this percentage with the symbol C/C_0, which expresses the percentage of these bonds in the film divided by their percentage in the film deposited in vacuum. The values of the ratio C/C_0 were obtained from XPS spectroscopy measurements [10, 11].

By comparing Fig. 5 with Fig. 6 we notice that, in the case of the B series, when the ratio C/C_0 increases, the peak position shifts toward higher wavenumbers (the hydrogen bonds become weakens). In the case of A series, the opposite occurs, as the peak position shifts toward lower wavenumbers (the hydrogen bonds become stronger). To explain this interesting result, we studied the S peak position as a function of the ratio C/C_0 (Fig. 7).

In Fig. 7, the point on the left belongs to the sample **i**, which has the highest bonds order degree [10, 11]. By examining the value of the spectral width of the D peak (Fig. 4) for each point in Fig. 7, we notice that, with the exception of the point for sample **i**, any shift of the S peak position towards higher wavenumbers is accompanied by an increase in the spectral width of the D peak. In addition, it appears from Fig. 7 that all points from the two series located within the range 0.5–1.1 on the ratio C/C_0 axis belong to the parabola shown in the figure. Accordingly, in the right part of the

parabola, any increase in the ratio C/C_0 will be associated with a decrease in both the S peak position and the spectral width of the D peak. In this case, the hexagonal rings become less distorted, and the gaps between them decrease, which in turn causes an increase in the strength of the hydrogen bonds that connect the water molecules to the surface of the film. Furthermore, In our previous work [11], we found that, all series A samples have a structure composed mostly of hexagonal rings [11], and as shown in Fig. 7, all points of these samples lie on the parabola with a high correlation coefficient ($R^2 = 0.999$). This result indicates that the effect of both the Csp^2-Csp^2 bonds concentration and the degree of distortion appears clearly in structures composed mainly of hexagonal rings. The results we obtained regarding the S peak position also apply to the case of W peak.

Figure 8 displays the intensity of the S peak (relative area) as a function of the ratio C/C_0. We notice that the intensity behaves similar to the position in Fig. 7, where it increases with the increase in the spectral width of the D peak in the Raman spectrum for both types of samples. One exception to this rule occurs when moving from the point corresponding to sample **f** to the point corresponding to sample **g**. The reason for this is that sample **f** may have a high percentage of nitrogen atoms bonded to carbon atoms by sp^3 hybridization [12], which makes its structure more branched. However, it is noted that the use of nitrognen plasma leads to an increase in the percentage of water molecules attached to the film surface for low and high values of the ratio C/C_0. In the case of medium values, the use of molecular nitrogen accompanied by an effective increase in this ratio.

The electrical conductivity of the film plays an important role in determining the bond strength between the adsorbed water molecules and the film surface. Therefore, we studied the relationship between the intensity of the S peak and the optical energy band gap of the film (Fig. 9). By tracing the distribution of the experimental points from left to right in Fig. 9, we notice that the proportional relationship between the S peak position and the D peak spectral width remains true only in the case of series B samples. It must be mentioned here that the structure of the samples of this series contains important proportions of carbon chains [11]. On the other hand, the reason the proportionality rule was not met in the case of A-series samples may be that the energy band gap is not only related to the ratio C/C_0, but is affected by many other factors, especially in samples with structures consisting of hexagonal rings.

(The optical energy band gap was estimated using Tauc method [21] and this has been documented in previous work [22]).

Finally, what draws attention when comparing Figs. 8 and 9 is the distorted mirror image symmetry between the curves of each series A and B. This is due to the different type of proportionality that determines the relationship between the electrical conductivity of the film and both the energy band gap and the ratio C/C_0.

4 Conclusions

Thin amorphous carbon nitride films were prepared by ablation of graphite targets using a pulsed laser in two different gases: the first was molecular nitrogen gas and the second was nitrogen plasma. After that, we characterized the resulting films using several spectroscopes, including FTIR spectroscopy, with the aim of investigating the effect of preparation conditions on water adsorption on the prepared films. The results obtained showed the following:

1. Increasing molecular nitrogen pressure reduces the humidity of amorphous carbon nitride films.

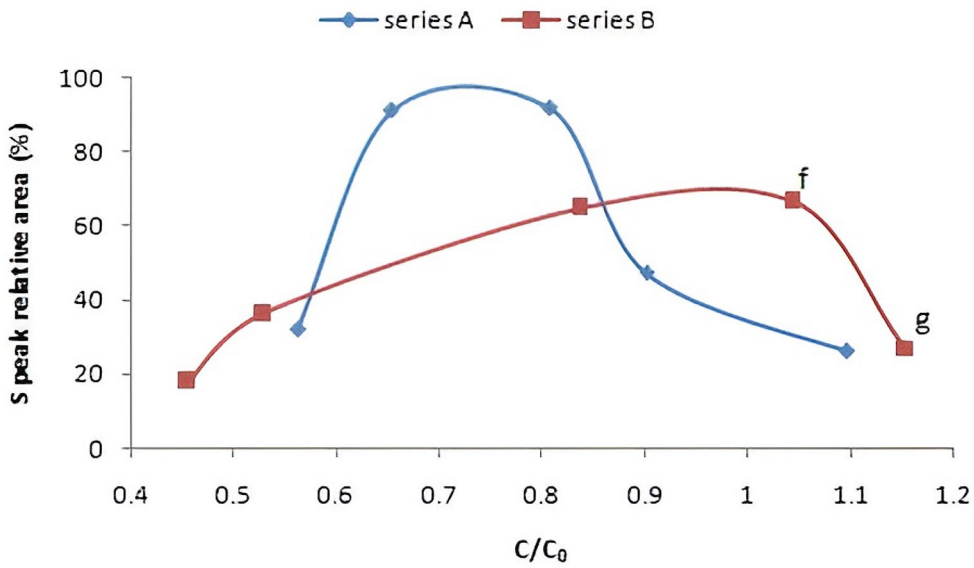

Fig. 8 The S peak relative area as a function of the ratio C/C_0

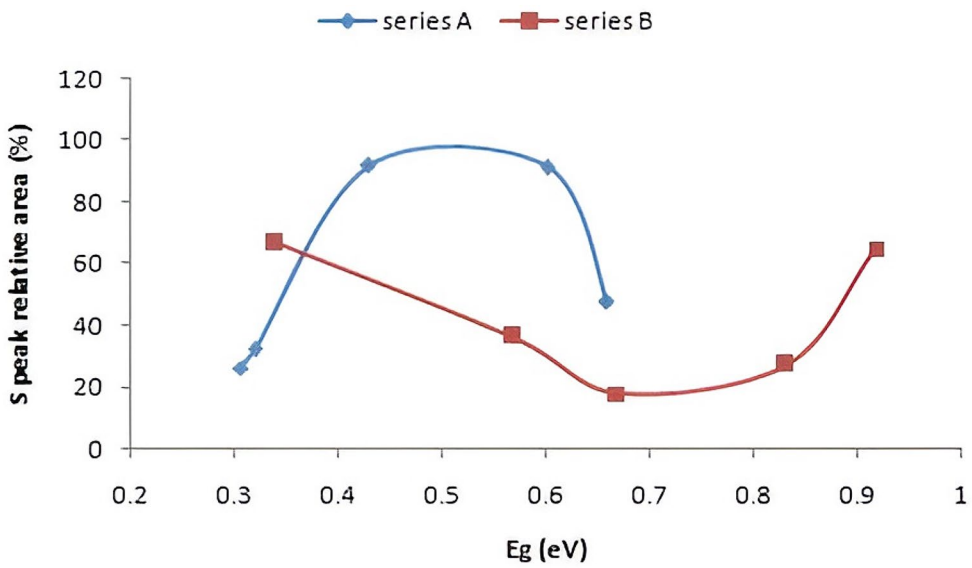

Fig. 9 The S peak relative area as a function of the energy band gap

2. The use of nitrogen plasma significantly affects the relationship between water adsorption and desorption pressure.
3. The effect of Csp^2-Csp^2 bonds concentration (the ratio C/C_0) on the adsorption of water molecules depends greatly on the ratio and distortion of the hexagonal rings.
4. The relationship between the hydrogen bonding strength of water molecules with the film surface and the concentration of Csp^2-Csp^2 bonds takes a specific mathematical formula in the case of structures composed mainly of hexagonal rings.
5. The use of nitrogen plasma leads to an increase in the percentage of water molecules attached to the film surface for low and high values of the ratio C/C_0.
6. The relationship between the S peak intensity and the ratio C/C_0 has distorted mirror symmetry with the relationship between the S peak intensity and the energy band gap.

Acknowledgements The author would like to thank Professor I. Othman, the Director General of Syrian Atomic Energy Commission for encouragement and support. The author would also like to thank Dr. (A) Alkhawwam, and Dr. (B) Abdallah for their assistance.

Author contributions Kamal Kayed wrote the main manuscript text, prepared all figures and reviewed the manuscript.

Funding Not applicable.

Data availability No datasets were generated or analysed during the current study.

Declarations

Ethical approval This is an observational study. No ethical approval is required.

Consent for publication Not applicable.

Consent to participate Not applicable.

Conflict of interest Not applicable.

References

1. Broitman, E., Gueorguiev, G.K., Furlan, A., Son, N.T., Gellman, A.J., Stafström, S., et al.: Water adsorption on fullerene-like carbon nitride overcoats. Thin Solid Films. **517**, 1106–1110 (2008). https://doi.org/10.1016/j.tsf.2008.07.022
2. Broitman, E., Gueorguiev, G.K., Furlan, A., Son, N.T., Gellman, A.J., Stafström, S., Hultman, L.: Water adsorption on fullerene-like carbon nitride overcoats. Thin Solid Films. **517**(3), 1106–1110 (2008)
3. Sayari, A., Belmabkhout, Y.: Stabilization of amine-containing CO2 adsorbents: Dramatic effect of water vapor. J. Am. Chem. Soc. **132**, 6312–6314 (2010)
4. Wiederhorn, S.: Influence of water vapor on crack propagation in soda-lime glass. J. Am. Ceram. Soc. **50**, 407–414 (1967)
5. Date á: Haruta á. Moisture effect on CO oxidation over Au/TiO 2 catalyst. J. Catal. **201**, 221–224 (2001)
6. Zahab, A., Spina, L., Poncharal, P., Marliere, C.: Water-vapor effect on the electrical conductivity of a single-walled carbon nanotube mat. Phys. Rev. B. **62**, 10000 (2000)
7. Jung, I., Dikin, D., Park, S., CaiW, Mielke, S.L., Ruoff, R.S.: Effect ofwater vapor on electrical properties of individual reduced graphene oxide sheets. J. Phys. Chem. C. **112**, 20264–20268 (2008)
8. Masami Aono, M., Terauchi, Y.K., Sato, K., Morita, T., Inoue, K., Kanda, K., Yonezawa: Deposition of amorphous carbon nitride thin films using pressure-gradient RF magnetron sputtering and their chemical bonding structures. Appl. Surf. Sci. **635**, 157677 (2023)

9. Matthews, A., Eskildsen, S.S.: Engineering applications for diamond-like carbon, Diamond and Related Materials, **3**, (4–6), 902–911, (1994)
10. Kayed, K.: Effect of nitrogen plasma afterglow on the (1000–1800) cm^{-1} band in FTIR spectra of amorphous carbon nitride thin films. Spectrochim Acta Mol. Biomol. Spectrosc. **190**, 253–258 (2018)
11. Kayed, K.: Effect of nitrogen plasma afterglow on the surface charge effect resulted during XPS surface analysis of amorphous carbon nitride thin films. Spectrochim Acta Mol. Biomol. Spectrosc. **199**, 242–247 (2018)
12. Alkhawwam, A., Abdallaha, B., Kayed, K., Alshoufi, K.: Effect of nitrogen plasma afterglow on amorphous carbon nitride thin films deposited by laser ablation. Acta Phys. Pol. A. **120**, 545–551 (2011)
13. Bezrodna, T., Puchkovska, G., Shymanovska, V., Baran, J., Ratajczak, H.: IR-analysis of H-bonded H_2O on the pure TiO2 surface. J. Mol. Struct. **700**, 175–181 (2004)
14. Hind, A., Al-Abadleh, Grassian, V.H.: FT-IR study of Water Adsorption on Aluminum Oxide surfaces. Langmuir. **19**, 341–347 (2003)
15. Lumeng, Liu: Shiliang (Johnathan) Tan, Toshihide Horikawa, D.D. Do, D. Nicholson, Junjie Liu, Water adsorption on carbon - A review, Advances in Colloid and Interface Science, **250**, 64–78, (2017)
16. Rahman, M.Z., Tapping, P.C., Kee, T.W., Smernik, R., Spooner, N., Moffatt, J., Tang, Y., Davey, K., Qiao, S.Z.: A Benchmark Quantum Yield for Water Photoreduction on Amorphous Carbon Nitride. Adv. Funct. Mater. 271702384 (2017). https://doi.org/10.1002/adfm.201702384
17. Wu, H.-Z., Liu, L.-M., Zhao, S.-J.: The effect of water on the structural, electronic and photocatalytic properties of graphitic carbon nitride. Phys. Chem. Chem. Phys. **16**, 3299 (2014)
18. Chengyong Wang, Y., Xing, Y., Lei, Y., Xia, C., Zhang, R., Zhang, S., Wang, P., Chen, S., Zhu, J., Li, X., Gui: Adsorption of water on carbon materials: Adsorption of water on carbon materials: The formation of water bridge and its effect on water adsorption. Colloids Surf. A: Physicochemical Eng. Aspects Volume **631**, 2021,127719
19. Toshihide Horikawa, T., Muguruma, D.D., Do, K.-I., Sotowa, J.: Rafael Alcántara-Avila, scanning curves of water adsorption on graphitized thermal carbon black and ordered mesoporous carbon. Carbon. **95**, 137–143 (2015)
20. Tan Xing, L.H., Li, L., Hou, X., Zhou, H.S., Peter, R.: Mladen Petravic, Ying Chen, Disorder in ball-milled graphite revealed by Raman spectroscopy. Carbon Volume. **57**, 515–519 (2013)
21. Mott, N.F., Davis, E.A.: Electronic Properties in Non-crystalline Materials. Oxford University Press, London (1971)
22. Kamal Kayed: The optical band gap in amorphous carbon nitride thin films: Effect of sp^2 hybridized C atoms configurations, fullerenes, nanotubes and Carbon Nanostructures, **27**:10, 796–802, (2019). https://doi.org/10.1080/1536383X.2019.1648438